JOURNAL OF AIRCRAFT
Vol. 31, No. 3, May–June 1994

Active Control of Wing Rock Using Tangential Leading-Edge Blowing

G. S. Wong,* S. M. Rock,† N. J. Wood,‡ and L. Roberts§
Stanford University, Stanford, California 94305

Experiments were performed to demonstrate positive poststall roll control of a free-to-roll wind-tunnel delta wing model using tangential leading-edge blowing. Previous static experiments had shown that significant rolling moments could be produced up to an angle of attack of 55 deg using asymmetric tangential leading-edge blowing. The implication was that poststall dynamic roll control ought to be possible using only blowing. To demonstrate experimentally that this was indeed the case, a free-to-roll wind-tunnel model sting mounting system and a pair of fast acting blowing control servo-valves were developed and manufactured. An automatic feedback roll control algorithm using tangential leading-edge blowing was then synthesized and implemented on a digital controller. Results from the present dynamic experiments indicated that with just symmetric blowing alone, wing rock at an angle of attack of 55 deg was damped. Furthermore, with the use of an automatic roll feedback control algorithm employing asymmetric blowing, the same wing rock was stopped in less than one cycle of the limit-cycle oscillation.

Nomenclature

A_j = jet exit area
AR = wing aspect ratio, b^2/S_{ref}
b, c_r = wing span, wing root chord
C_l = rolling moment coefficient $\mathcal{L}/q_\infty S_{ref} b$
C_μ = blowing coefficient $\dot{m}_j V_j / q_\infty S_{ref}$
$C_{\mu.L}$ = left leading-edge blowing coefficient
$C_{\mu.R}$ = right leading-edge blowing coefficient
$C_{\mu.SYM}$ = symmetric blowing coefficient
$\mathcal{L}$ = aerodynamic rolling moment
$\dot{m}_j$ = jet mass flow rate $\rho_j V_j A_j$
q_∞ = tunnel dynamic pressure $\frac{1}{2}\rho U_\infty^2$
Re = Reynolds number $\rho U_\infty c_r / \mu$
S_{ref} = reference area, wing planform
U_∞ = tunnel freestream velocity
V_j = jet exit velocity
α_0 = angle of attack at zero sideslip and roll
$\Delta C_{\mu.L}$ = asymmetric blowing coefficient increment-left, $C_{\mu.L} - C_{\mu.SYM}$
$\Delta C_{\mu.R}$ = asymmetric blowing coefficient increment-right, $C_{\mu.R} - C_{\mu.SYM}$
Δp = plenum pressure above atmospheric
Λ = leading-edge sweep angle
ρ_j = jet air density
ϕ = wing roll angle

I. Introduction

RECENT studies[1–3] have suggested that significant air tactical advantage can be gained through poststall maneuvers. The anticipated need for effective vehicle and flowfield control capabilities during such violent maneuvers was also emphasized.[3] This study concentrates on the lateral control of the aircraft, more specifically, that of roll control about the longitudinal body axis at high angles of attack using a direct flowfield management technique.

The flow separation at the leading edges of a delta wing which results in the formation of leading-edge vortices on the lee-side of the wing is directly altered by tangential leading-edge blowing (TLEB) as depicted in Fig. 1. By means of the Coanda effect, the tangentially exiting jet is caused to remain attached around the rounded surface at the leading edge.[4] Through viscous interaction with the surface following Coanda jet, the boundary layer of the flow in the vicinity of the leading edge is energized and separation is delayed. The displaced flow separation point causes the affected leading-edge vortex to change in both position and strength in attaining a new equilibrium state. Depending on the amount of blowing, the position and strength of the leading-edge vortex, and therefore, the entire vortical flowfield is modified accordingly.

At angles of attack where the leading-edge vortex is burst, tangential leading-edge blowing partially reattaches the flow around the leading edge and allows the flow to separate in a manner such that formation of a strong leading-edge vortex is again possible.[5] By blowing symmetrically, i.e., blowing equally along both the left and the right leading edges, the burst leading-edge vortices at poststall angles of attack are unburst.[6,7] The total normal force of the wing is increased[6] due to the increased vortex suction from the unburst leading-edge vortices, and due to the increased leading-edge suction resulting from the partial flow attachment around the rounded leading edges.

Besides blowing symmetrically, it is also possible to blow asymmetrically, i.e., to introduce blowing along either the left or the right leading edge only. Asymmetric blowing results in the formation of an asymmetric vortical flowfield on the lee-side of the wing. The resultant asymmetric pressure distribution then produces a rolling moment, the magnitude of which is proportional to the amount of asymmetric blowing introduced.[6] An interesting phenomenon reported was that between prestall and poststall angles of attack, the rolling moment generated by asymmetric blowing had a change in sign.[6–8] This effect could potentially limit the usefulness of tangential leading-edge blowing as a roll control actuator in a maneuver where sudden rapid rotation to and from poststall

Received Oct. 17, 1992; presented as Paper 93-0056 at the AIAA 31st Aerospace Sciences Meeting, Reno, NV, Jan. 11–14, 1993; revision received Feb. 12, 1993; accepted for publication May 31, 1993.

*Ph.D., Department of Aeronautics and Astronautics; currently Control Systems Engineer, Advanced Product Development, Bird Products Corporation, 1100 Bird Center Drive, Palm Springs, CA 92262. Member AIAA.

†Associate Professor, Department of Aeronautics and Astronautics. Senior Member AIAA.

‡Research Associate, Department of Aeronautics and Astronautics; currently Senior Lecturer, School of Mechanical Engineering, University of Bath, Bath BA2 7AY, England, UK. Member AIAA.

§Professor, Department of Aeronautics and Astronautics. Fellow AIAA.

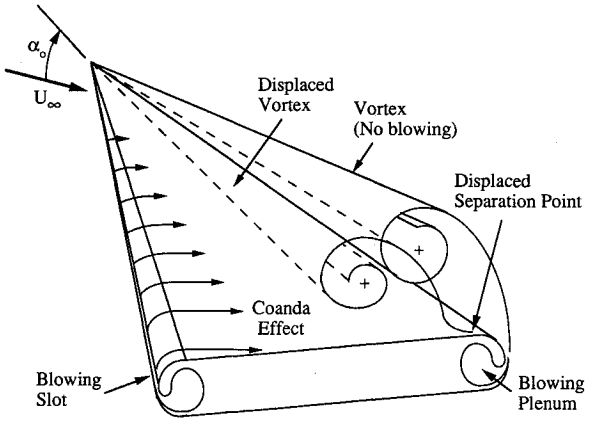

Fig. 1 Tangential leading-edge blowing.

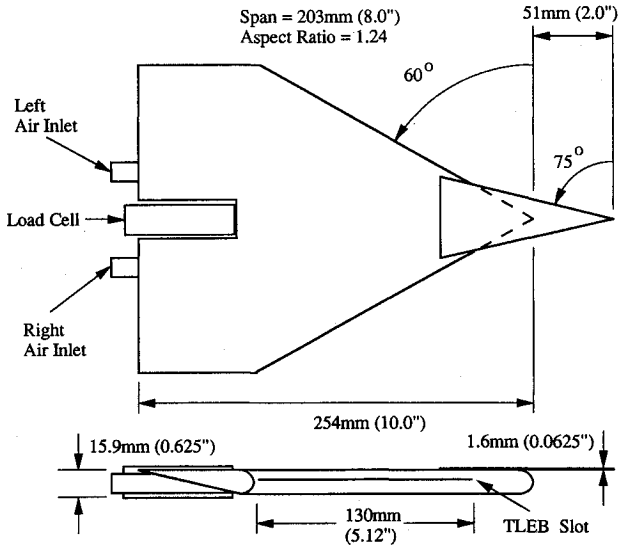

Fig. 2 Wind-tunnel delta wing model.

angles of attack is required. However, a method to eliminate this undesirable roll control reversal effect using symmetric blowing superimposed on asymmetric blowing is offered in the present study.

The primary objective of this study is to demonstrate experimentally the feasibility and usefulness of asymmetric tangential leading-edge blowing in controlling the roll dynamics of a delta wing at a poststall angle of attack where the leading-edge vortices are completely burst. Stabilization of wing rock which is caused by the unsteadiness of the flow over the wing[9] is presented in this article as an example of the capability of tangential leading-edge blowing.

II. Experiment

A. Wind-Tunnel Model

The present delta wing model was designed to be used in both static and dynamic experiments in Stanford's 0.46-m (18-in.) low-speed closed-circuit wind tunnel. It had no movable conventional control surfaces. The model had a span of 203 mm (8.0 in.) and a root-chord length of 305 mm (12.0 in.), resulting in AR = 1.24 (Fig. 2).

The relatively thin tip delta had sharp leading edges with a sweep angle of $\Lambda = 75$ deg, and was mounted directly on the upper surface above the apex of the much thicker cropped delta wing. In so doing, the atypical flow over and around the blunt apex of the relatively thick cropped delta wing at high angles of attack was corrected and vortical flow asymmetry was established, making wing rock possible. The cropped delta wing was of constant thickness, approximately 6% at the root chord, and had $\Lambda = 60$ deg. The trailing edge was made to have zero thickness by the inclusion of fixed tapered trailing-edge flaps.

The tangential leading-edge blowing slots extended from immediately aft of the tip delta to the wingtips along the leading edges of the cropped delta wing. For the present experiment, the slot width varied from 0.15 mm (0.006 in.) at the front to 0.43 mm (0.017 in.) at the wingtip over a distance of 130 mm (5.12 in.) along the leading edges. This variation produced a linear variation in blowing momentum over the wing, a configuration which had previously been shown to be efficient.[4]

A three component strain-gauge load cell measuring normal force, pitching moment, and rolling moment of the delta wing was installed between the model and the mounting sting. During dynamic experiments, this same load cell was used to measure the disturbance torque introduced by the supporting shaft and the ball bearings which held the shaft in place. A single low-friction linear conductive plastic potentiometer with negligible inertia was coupled to the end of the support shaft to measure the turning of the shaft, and hence, the roll angle of the wing (defined to be positive starboard wing down).

B. Blowing Control Valves

Two separate internal plena inside the delta wing model were used to channel the blowing supply air to the corresponding leading edges. During static experiments, plenum pressures were regulated down from a high-pressure [typically 482 kPa (70 psi)] shop air source using manual pressure regulators. Pressure transducers, located outside the tunnel, were connected to pressure tappings inside the blowing air plenum to monitor plenum pressures. Because of low flow rates, the internal plenum pressure [typically from 0 to 9.6 kPa (1.4 psi) above the ambient atmospheric pressure] Δp, was used to calculate the blowing momentum coefficient C_μ. Here

$$C_\mu = 2\frac{A_j}{S_{\text{ref}}}\left(\frac{V_j}{U_\infty}\right)^2 \tag{1}$$

where S_{ref} is the wing planform area. The jet velocity is calculated using the following equation:

$$V_j = \sqrt{2(\Delta p/\rho_j)} \tag{2}$$

where ρ_j is the constant jet air density (incompressible flow).

During dynamic experiments, high-speed rotary servo-valves installed just below the test section to minimize the distance between the servo-valves and the blowing plenum, were used in series with the manual valves to provide fast blowing plenum pressure regulation. A brushless dc motor, chosen for its low rotor inertia and internal friction, was coupled directly to each valve shaft via a bellows coupler. Valve angular position feedback was achieved by means of the linear conductive plastic potentiometer coupled directly to the rear of the motor. Operational-amplifiers were used to implement the proportional-derivative feedback compensator to achieve the highest possible response rate of the valve angle feedback control system.

The required blowing C_μ in a closed-loop feedback roll control system was achieved with the use of a separate plenum pressure feedback control loop. In this control loop, the necessary Δp as defined by Eqs. (1) and (2) was first determined. Then, by commanding the valve system to open to the precalibrated angle which corresponded to the necessary Δp, the required blowing was achieved.

C. Free-to-Roll Sting Mount

Tangential leading-edge blowing required the connection of air supply hoses to the wind-tunnel model. The presence of these hoses, if not compensated for, introduced enough of a disturbance torque (e.g., friction and torsional spring effect) to stop the wing from its natural rocking motion. The elimination of this disturbance torque was accomplished by means

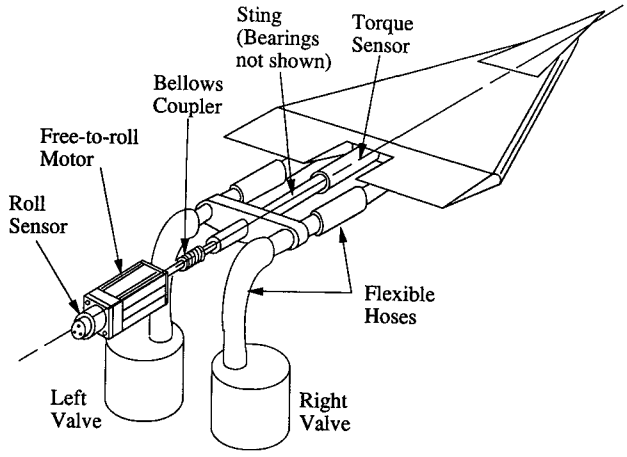

Fig. 3 Wing mounting configuration for roll control experiments with free-to-roll motor.

of a small brushless dc motor installed at the rear of the supporting shaft as shown in Fig. 3. A backlash-free bellows coupler was used to couple the motor to the shaft to eliminate end-play between the shaft and the motor.

Two control loops were implemented in an effort to eliminate all disturbances introduced by the air supply hoses.[10] The roll angle signal and the rolling moment torque signal were both used in the feedback control algorithm. The nonlinear spring effect of the air supply hoses was calibrated and then stored in the form of a look-up-table on the computer. During operation, this first feedback loop provided the necessary spring effect cancelling torque as a function of the wing roll angle. However, due to friction and nonlinearities in the free-to-roll motor, and due to air passing through the supply hoses (thus changing the effective spring constant of the hoses), this torque cancellation was imperfect. To minimize the residual disturbance torque, the signal from the torque sensor was used in a second feedback loop. A notch filter was incorporated in the second feedback control law in order to eliminate a resonance resulting from compliance in the torque sensor.

Performance of the control algorithm was evaluated by monitoring the torque signal measured with the load cell.[10] A torque signal of zero would mean no transmission of torque from the sting to the wing. This would be ideal. In actuality, the disturbance torque level during dynamic wing rock was kept to a level comparable to the torque level during free-to-roll wing rock (the disturbance torque in this case came mostly from the ball-bearings which held the supporting shaft in place) where no blowing hoses were attached, i.e., $|C_\ell| \leq 1.0 \times 10^{-3}$.

III. Results and Discussion

The result of the present research is presented in the following two sections. Effects of symmetric and asymmetric tangential leading-edge blowing on the static wing rolling moment behavior are presented in Sec. IV. Dynamic wing rock experiments and the result of active feedback control of wing rock using blowing are presented in Sec. V. Unless otherwise stated, all the results presented were of experiments conducted at an angle of attack of $\alpha_0 = 55$ deg, and at a wind-tunnel speed of $U_\infty = 20$ m/s (65.6 ft/s) which corresponded to a Reynolds number, based on the wing root chord of $R_c = 4.0 \times 10^5$.

IV. Static Experiments

A. Effects of Symmetric Blowing

The rolling moment generated as a result of side-slip caused by the rolling of the wing about its longitudinal axis was measured using the strain-gauge load-cell located between the wing and the supporting sting as shown in Fig. 2. The effects

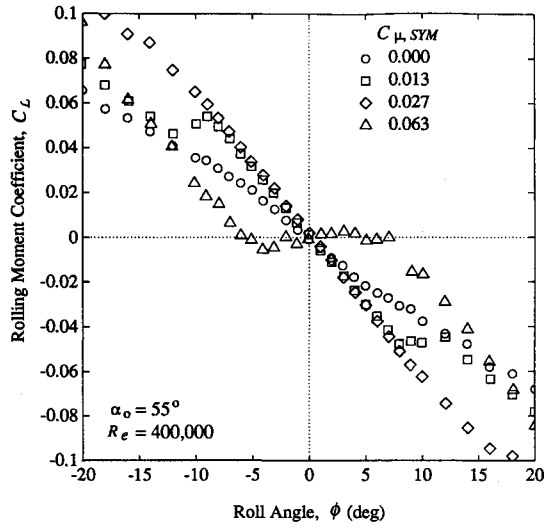

Fig. 4 Effects of symmetric blowing on wing rolling moment coefficient $C_{\mu,SYM}$ = 0.000, 0.013, 0.027, 0.063.

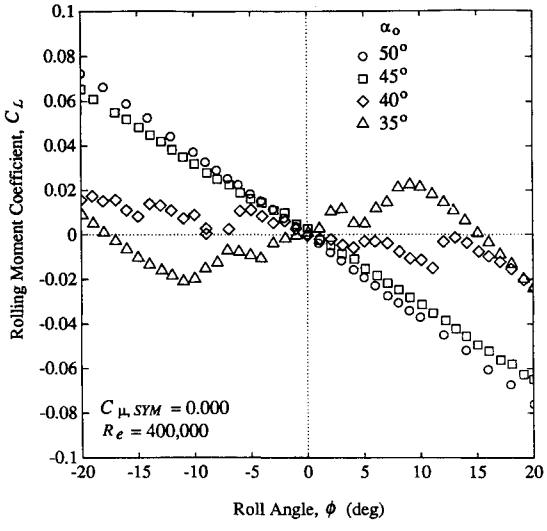

Fig. 5 Effects of varying angle of attack on wing rolling moment coefficient $C_{\mu,SYM}$ = 0.000, α_0 = 50, 45, 40, 35 deg.

of increasing symmetric blowing on the static wing C_ℓ are presented in Fig. 4. As shown, with increasing symmetric blowing from no blowing, there was an initial increase in the slope of the C_ℓ vs ϕ curve. One could think of the rolling moment generated as that by an aerodynamic torsional spring. Then an increase in the slope of the C_ℓ vs ϕ curve is equivalent to an increase in the stiffness of the aerodynamic spring, or *roll stiffness* of the wing.

For $C_{\mu,SYM} = 0.013$, dramatic changes in the rolling moment coefficient with changes in the roll angle were observed. The nonlinearities in the C_ℓ vs ϕ data were caused by an asymmetric unbursting of the leading-edge vortices, i.e., the unbursting of the leading-edge vortex on the leeward side of the wing and not on the windward side for positive roll angles. Positive sideslip reduces the sweep angle of the windward leading edge (hence, moving the windward vortex burst location forward), while increasing the sweep of the leeward leading edge (hence, moving the leeward burst location aft). Since both leading-edge vortices are initially burst at zero sideslip, positive sideslip here can only lead to an unbursting of the leeward vortex by moving the leeward burst location aft toward the trailing edge of the wing.[11] The net effect is a leeward wing up, or a positive increment to the wing rolling moment.

A symmetric blowing value of $C_{\mu,SYM} = 0.027$ significantly reduced the nonlinearities while maintaining the roll stiffness

of the wing. However, with further increase in symmetric blowing, not only was there a decrease in the roll stiffness of the wing, the slope became zero and then changed sign with $C_{\mu,\mathrm{SYM}} = 0.063$. This slope reversal of the C_l vs ϕ data was observed for the same wing when the angle of attack was decreased from $\alpha_0 = 55$ deg. Plotted in Fig. 5 are the C_l vs ϕ data for the wing at $\alpha_0 = 50$, 45, 40, and 35 deg without any blowing. As shown, the wing appeared to be neutrally stable in roll at $\alpha_0 = 40$ deg, and became unstable in roll about $\phi = 0$ deg at $\alpha_0 = 35$ deg. Note that at $\alpha_0 = 35$ deg, the wing had stable roll equilibrium points at $\phi \approx \pm 18$ deg. The dynamic rocking behavior of the wing about these equilibrium points, though interesting, was beyond the scope of this research, and therefore was not studied in any detail. But what was evident from the above data was the similarities in the wing rolling moment behavior between an increase in the symmetric blowing amount at a poststall angle of attack, and a decrease of the angle of attack from a poststall angle of attack. In summary, increasing symmetric blowing at a poststall angle of attack of $\alpha_0 = 55$ deg had an effect on the lateral directional characteristics of the wing which was similar to decreasing the effective angle of attack of the wing.

The fundamental physics responsible for the above observation was the unbursting of the leading-edge vortices at poststall angles of attack due to symmetric blowing. An increase in symmetric blowing causes a decrease in the effective angle of attack of the wing. Flow visualization pictures[10] showed that the burst vortical flow at an angle of attack of 50 deg could be made to resemble that at an angle of attack of 30 deg with the use of an appropriate amount of symmetric blowing. It was also possible to attach fully the flow over the delta wing at poststall using symmetric blowing. The vortical flow in which case would be absent and the effective angle of attack would be 0 deg, even though the actual angle of attack was 55 deg.

B. Effects of Asymmetric Blowing

Asymmetric blowing in the present research was accomplished by increasing the blowing along either the left leading edge or the right leading edge above the symmetric blowing level. For example, increasing the asymmetric blowing on the right meant increasing blowing on the right (starboard) side of the wing while keeping the blowing on the left (port) side constant. Specifically

$$\Delta C_{\mu,R} = C_{\mu,R} - C_{\mu,\mathrm{SYM}} \tag{3}$$

$$\Delta C_{\mu,L} = C_{\mu,L} - C_{\mu,\mathrm{SYM}} \tag{4}$$

Note $\Delta C_{\mu,R} \geq 0$ and $\Delta C_{\mu,L} \geq 0$ always. Furthermore, when $\Delta C_{\mu,R} > 0$, $\Delta C_{\mu,L} = 0$ and vice versa.

The asymmetric blowing rolling moment responses with no superimposed symmetric blowing $C_{\mu,\mathrm{SYM}} = 0.000$, superimposed symmetric blowing of $C_{\mu,\mathrm{SYM}} = 0.027$, and 0.053 are shown in Fig. 6. Plotted along the abscissa are the asymmetric blowing values, positive for asymmetric blowing right and negative for asymmetric blowing left. Plotted along the ordinate are the rolling moment coefficients. In addition to the asymmetric blowing rolling moment responses at a roll angle of $\phi = 0$ deg, asymmetric blowing rolling moment responses at roll angles of $\phi = \pm 6$ deg for $C_{\mu,\mathrm{SYM}} = 0.000$, and $\phi = \pm 10$ deg for $C_{\mu,\mathrm{SYM}} = 0.027$ and 0.053 are also included.

The rolling moment responses at $\phi = 0$ deg confirmed what was observed in Refs. 6–8. Asymmetric blowing on the left initially gave negative, or left wing down rolling moment. With large amounts of asymmetric blowing, the rolling moment changed sign, i.e., left asymmetric blowing then gave a positive, or left wing up rolling moment. The above observations were caused by the vortical flow cross-coupling effects at poststall angles of attack as described in Ref. 6. Specifically, it was observed that at a poststall angle of attack of 50 deg, blowing on the left enhanced first the vortex on the right. The result was a negative, or left wing down initial rolling moment. Further increasing the blowing on the left then unburst the vortex on the left, causing the rolling moment to become more positive. The unburst left leading-edge vortex together with the increased leading-edge suction force along the left leading edge eventually caused the rolling moment to become positive. A discussion on the factors which could influence the cross-coupling can also be found in the reference cited above.

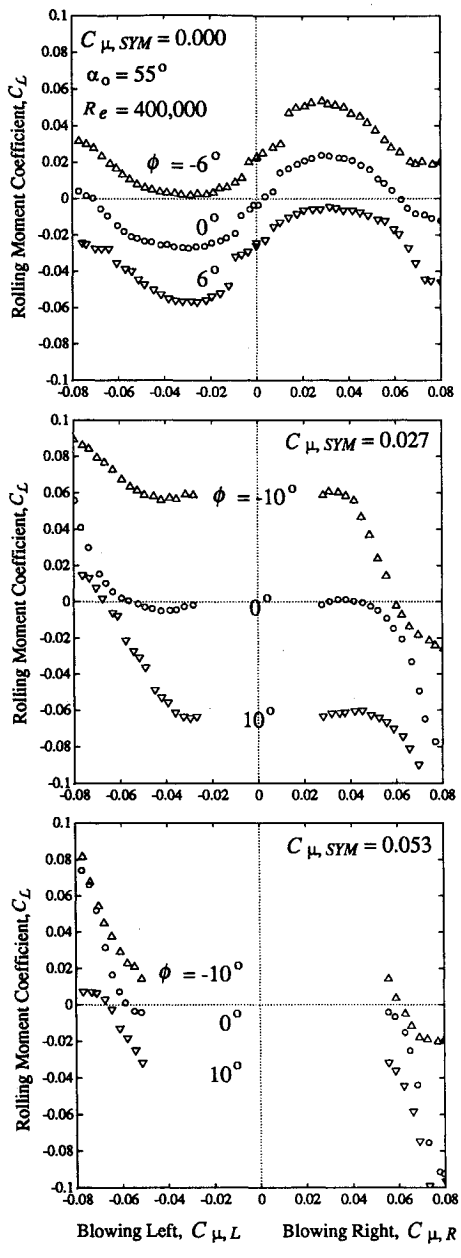

Fig. 6 Effects of asymmetric blowing on wing rolling moment $C_{\mu,\mathrm{SYM}}$ = 0.000, 0.027, 0.053.

In addition to the sign reversal phenomenon addressed above, it can also be seen that with whatever amount of asymmetric blowing, no zero crossing of the rolling moment response is possible for roll angles $|\phi| = 6$ deg (Fig. 6). The implication is that the wing just cannot be statically trimmed in roll at roll angles $|\phi| > 6$ deg using asymmetric blowing if $C_{\mu,\mathrm{SYM}} = 0.000$.

As mentioned above, with the use of superimposed symmetric blowing, blowing values less than the symmetric blowing value were not used. In addition, the blowing opposite the asymmetric blowing side was kept at the symmetric blowing value. This implementation of asymmetric blowing resulted in the gaps between the asymmetric blowing right and the asymmetric blowing left data seen in the above figures.

With increasing superimposed symmetric blowing, the rolling moment sign reversal happened with less and less asymmetric blowing. For an initial symmetric blowing value of $C_{\mu.SYM} = 0.053$, no sign reversal was observed. The rolling moment characteristics shown in Fig. 6 for $C_{\mu.SYM} = 0.027$ resembled that at a prestall angle of attack of $\alpha_0 = 30$ deg with no symmetric blowing superimposed.[6-8] Hence, with the introduction of superimposed symmetric blowing at a poststall angle of attack, the asymmetric blowing roll control reversal problem between prestall and poststall angles of attack was eliminated. In addition, the maximum trimmable roll angle was increased from $|\phi| = 6$ deg for $C_{\mu.SYM} = 0.000$ to $|\phi| = 10$ deg for $C_{\mu.SYM} = 0.027$ and 0.053. Another benefit of the use of superimposed symmetric blowing was the linearization of the asymmetric blowing rolling moment responses. The higher the rate of superimposed symmetric blowing, the more linear the asymmetric blowing rolling moment responses become.

V. Dynamic Experiments

A. Wing Rock

The phenomenon of wing rock has been observed and studied quite extensively and various explanations for its occurrence have been proposed in the past.[9,12] This self-induced roll instability observed for the present delta wing model is shown in Fig. 7. These data are for the wing with no air supply hoses and no free-to-roll motor attached.

The steady-state amplitude and frequency of the present wing rock was approximately 8 deg and 2 Hz, respectively.

B. Effects of Symmetric Blowing on Wing Rock

The damping effect of symmetric blowing on wing rock is presented in Fig. 8. These data are for the wing with the air supply hoses and the free-to-roll motor attached as shown in Fig. 3. In the case shown, symmetric blowing was introduced and held constant while the wing was undergoing wing rock. As shown, wing rock was attenuated with the use of symmetric blowing alone. The observed behavior was that with a larger amount of symmetric blowing, the attenuation of wing rock becomes more rapid. The small amplitude limit-cycling after the damping out of wing rock observed for $C_{\mu.SYM} = 0.043$ was caused by the residual disturbance torque in the free-to-roll system, the amplitude of which was comparable to the aerodynamic rolling moment only at very small roll angles.

The use of even larger amounts of symmetric blowing for faster damping of wing rock was prevented by static roll instabilities near $\phi = 0$ deg. Therefore, the rate of increasing attenuation of wing rock with the use of increasing amounts of symmetric blowing is limited. A method to increase the rate of attenuation by means of an automatic feedback control system is the topic of discussion in the following section.

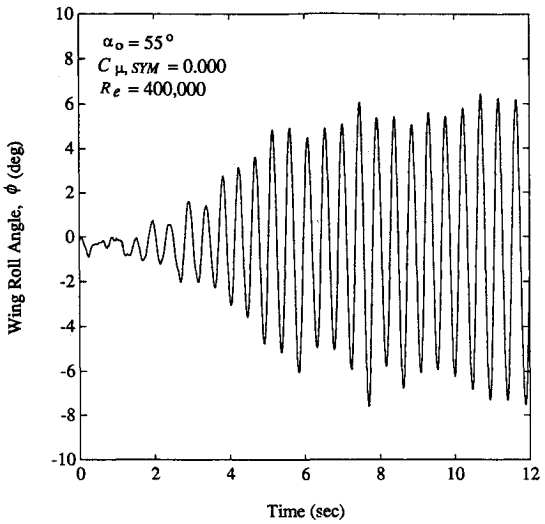

Fig. 7 Wing rock captured in the present experiment.

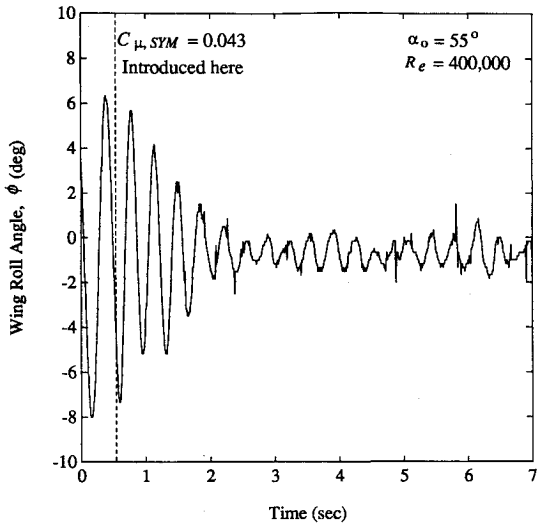

Fig. 8 Effects of symmetric blowing on wing rock $C_{\mu.SYM} = 0.043$.

C. Active Control of Wing Rock

The approach chosen in using TLEB for controlling wing rock consisted of a constant amount of symmetric blowing superimposed on top of the asymmetric blowing. The amount of asymmetric blowing was modulated in response to the measured wing rolling motion. The effects of the particular choice of superimposed symmetric blowing $C_{\mu.SYM} = 0.027$ on the wing static and dynamic characteristics are listed below.

1) The wing static rolling moment vs roll angle characteristic was linearized, i.e., there were no sudden bends or jumps in the C_l vs ϕ curve (Fig. 4, $C_{\mu.SYM} = 0.027$).

2) Aerodynamic damping was increased and wing rock was attenuated, e.g., Fig. 8.

3) The actuator characteristic, i.e., asymmetric blowing rolling moment response, was somewhat linearized. The absolute value of the static trimmable roll angles was greater than the wing rock amplitude (Fig. 6, $C_{\mu.SYM} = 0.027$).

An important observation was that for the symmetric blowing value chosen, the wing was already stable statically and dynamically in roll. Although the resulting system was far from being ideal, with the assumption that the actuator characteristics were perfectly linear and that the speed of response of the aerodynamic rolling moment to changes in blowing was infinitely fast,[13] the control problem reduced to a classical double-integrator problem. Stability was guaranteed with the use of an appropriate proportional-derivative compensator in the roll angle feedback loop. The control logic using asymmetric and superimposed symmetric blowing reflecting this design approach is shown in a block-diagram form in Fig. 11.

The control law design was implemented digitally. A difference equation of the proportional-derivative compensator was generated from the transfer function using the zero-order-hold method which then was programmed in the C language on an IBM-AT compatible Intel 80386/387 machine equipped with a data acquisition and control plug-in board. Assembly language C-callable subroutines were used to interface the computer to the data acquisition/control board to allow for high sampling rate digital closed-loop control.

The performance of the control system and the effects of the ignored nonlinearities on the closed-loop dynamic response are shown in Fig. 9. Wing rock was damped out in less than one cycle of the limit-cycle motion. The small amplitude limit-cycling about $\phi = 0$ deg was caused by a combination of a residual torque disturbance in the free-to-roll system and by the nonlinearities in the asymmetric blowing characteristics as shown in Fig. 6.

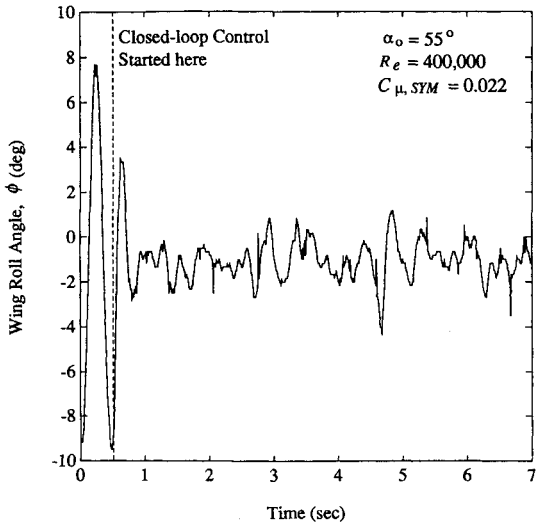

Fig. 9 Active control of wing rock using asymmetric TLEB.

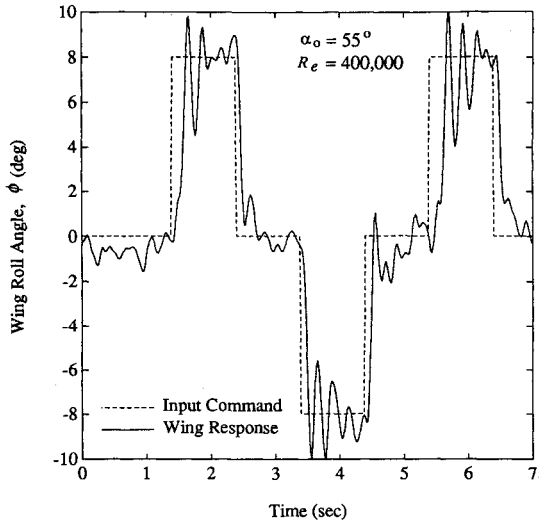

Fig. 10 Closed-loop response to roll command without gain-scheduling.

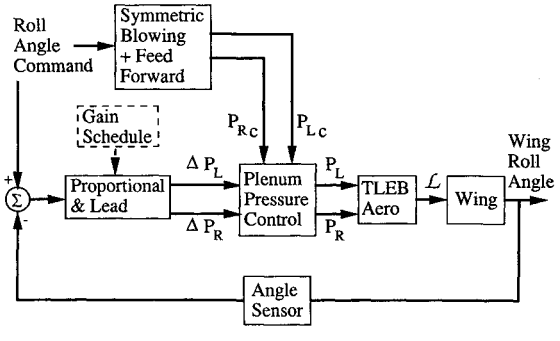

Fig. 11 Wing roll angle control logic.

D. Roll Command Following

It was possible to trim the wing at $\phi \neq 0$ deg at a poststall angle of attack using asymmetric blowing as mentioned earlier. With a command feed-forward control algorithm, the wing trim angle vs asymmetric blowing data of Fig. 6 were implemented in the form of a look-up-table. The resulting closed-loop response of the system to a square wave type roll angle command input signal of $\phi = \pm 8$ deg is shown in Fig. 10. The oscillations about $\phi = 0$ deg were as before. However, dynamic oscillations and large overshoots at the commanded roll angles of $\phi = \pm 8$ deg are evident. This was expected because of a gradual increase in sensitivity of the wing to

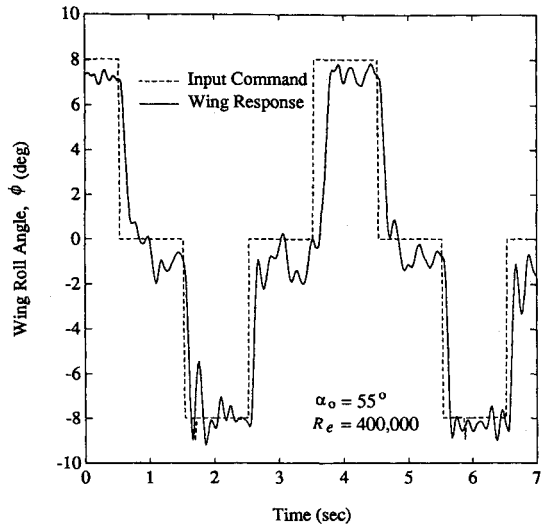

Fig. 12 Closed-loop response to roll command with gain-scheduling.

asymmetric blowing with increasing roll angles.[10] The control gains designed for use at zero roll angle therefore became too high at larger roll angles. By scheduling the control gains according to the sensitivity of the wing to asymmetric blowing, the overshoots were attenuated. A block diagram of the control algorithm with command feed-forward and the added gain-scheduling algorithm (dashed block) is shown in Fig. 11. The resulting closed-loop behavior is shown in Fig. 12. As shown, the dynamic oscillations and large overshoots at $\phi = \pm 8$ deg were greatly attenuated and roll angle command following was successfully demonstrated.

VI. Concluding Remarks

In this study, poststall roll control using tangential leading-edge blowing was demonstrated experimentally in a wind tunnel on a delta wing model which exhibited wing rock. The damping effect of symmetric blowing alone on wing rock was found to be effective up to a certain maximum blowing rate. The use of symmetric blowing above this limit resulted again in roll instabilities. A moderate amount of superimposed symmetric blowing was found to be effective in linearizing the asymmetric blowing static rolling moment responses. Control reversal between prestall and poststall angles of attack found previously was also eliminated. The use of asymmetric blowing at poststall attitudes for roll control thus became similar to the use of ailerons at prestall angles of attack. With the help of an active roll feedback control algorithm employing a proportional-derivative compensator, wing rock at a poststall angle of attack was stopped in less than one cycle of the limit-cycle motion using asymmetric blowing. Furthermore, roll command following was demonstrated with the use of a feed-forward gain-scheduling control algorithm.

Acknowledgments

This work was supported in part by NASA Ames under Grant NCC2-55. The authors would like to thank John Mohun, Robert Bower, Thomas Hasler, and Matthew Chuck in the Stanford Aero/Astro Machine Shop for their care and skills in fabricating the experimental setup; Marc Ullman in the Stanford Aerospace Robotics Lab for writing the assembly language C-callable digital control subroutines; Godwin Zhang also in the Aerospace Robotics Lab for his expert assistance in analog electronics; J. David Powell for his guidance in the development of the servo-valve control system; and finally Zeki Celik and Vadim Matte for their invaluable assistant during the various wind-tunnel tests.

References

[1]Herbst, W. B., "Future Fighter Technologies," *Journal of Aircraft*, Vol. 17, No. 8, 1980, pp. 561–566.

[2]Herbst, W. B., "Dynamics of Air Combat," *Journal of Aircraft*, Vol. 20, No. 7, 1983, pp. 594–598.

[3]Lang, J. D., and Francis, M. S., "Unsteady Aerodynamics—Fundamentals and Applications to Aircraft Dynamics," AGARD CP-386, April 1985.

[4]Wood, N. J., and Roberts, L., "The Control of Vortical Lift on Delta Wings by Tangential Leading Edge Blowing," *Journal of Aircraft*, Vol. 25, No. 3, 1988, pp. 236–243.

[5]Wood, N. J., Roberts, L., and Lee, K. T., "The Control of Vortical Flow on a Delta Wing at High Angles of Attack," AIAA Paper 87-2278, Aug. 1987.

[6]Wood, N. J., Roberts, L., and Celik, Z., "The Control of Asymmetric Vortical Flows over Delta Wings at High Angles of Attack," *Journal of Aircraft*, Vol. 27, No. 5, 1990, pp. 429–435.

[7]Celik, Z., and Roberts, L., "An Investigation of Asymmetric Vortical Flows over Delta Wings with Tangential Leading-Edge Blowing at High Angles of Attack," AIAA Paper 90-103, Jan. 1990.

[8]Wood, N. J., "Development of Lateral Control on Aircraft Operating at High Angles of Attack," 17th ICAS Meeting, Stockholm, Sweden, Aug. 1990.

[9]Nelson, R. C., "Unsteady Aerodynamics of Slender Wings," AGARD Special Course on Aircraft Dynamics at High Angles of Attack: Experiments and Modelling, AGARD-R-776 (N91-22105), March 1991.

[10]Wong, G. S., "Experiments in the Control of Wing Rock at High Angle of Attack Using Tangential Leading Edge Blowing," Ph.D. Dissertation, Dept. of Aeronautics and Astronautics, Stanford Univ., Stanford, CA, Dec. 1992.

[11]Greenwell, D. I., and Wood, N. J., "Control of Asymmetric Vortical Flows," AIAA Paper 91-3272, Sept. 1991.

[12]Ericsson, L. E., "The Fluid Mechanics of Slender Wing Rock," *Journal of Aircraft*, Vol. 21, No. 5, 1984, pp. 322–328.

[13]Wood, N. J., Lee, K. T., and Roberts, L., "Dynamic Control of Vortical Flow on Delta Wings at High Angles of Attack," AIAA Paper 88-4333, Aug. 1988.